Shining Light on Dark Matter, One Photon at a Time

by

Brandon Leigh Allen

Submitted to the Department of Physics
in partial fulfillment of the requirements for the degree of

Doctorate of Science in Physics

at the

MASSACHUSETTS INSTITUTE OF TECHNOLOGY

June 2019

Author . . . .
Department of Physics
May 18, 2019

Certified by . . . .
Christoph E.M. Paus
Professor
Thesis Supervisor

Accepted by . . . .
Nergis Mavalvala
Associate Department Head for Education

Shining Light on Dark Matter,

One Photon at a Time

by

Brandon Leigh Allen

Submitted to the Department of Physics
on May 18, 2019, in partial fulfillment of the
requirements for the degree of
Doctorate of Science in Physics

Abstract

A search is conducted for new physics in final states containing a photon and missing transverse momentum in proton-proton collisions at $\sqrt{s} = 13$ TeV. The data collected by the CMS experiment at the CERN LHC correspond to an integrated luminosity of 35.9 inverse femtobarns. No deviations from the predictions of the standard model are observed. The results are interpreted in the context of dark matter production and limits on new physics parameters are calculated at 95% confidence level. For the two simplified dark matter production models considered, the observed (expected) lower limits on the mediator masses are both 950 (1150) GeV for 1 GeV dark matter mass.

Thesis Supervisor: Christoph E.M. Paus
Title: Professor

Acknowledgments

This is the acknowledgements section. You should replace this with your own acknowledgements.

Contents

Chapter 1

Global Event Reconstruction

In the previous chapter, we discussed the interactions of particles with the individual subdetectors and how these generate electrical signals. Now, we shall discuss the reverse process, namely reconstructing the individual particles or physics objects from the electrical signals recorded by the subdetectors.

Traditionally, each class of physics object was reconstructed using information from a single subdetector: muons from the muon chambers, isolated photons and electrons from the ECAL, jets and missing transverse energy from the HCAL, and secondary vertices from τ lepton and b hadron decays from the tracker. However, as depicted in Figure 1-1, each type of particle interacts with multiple different subdetectors and this information is lost unless the information from all the subdetectors is combined into a single global event description.

The particle flow (PF) algorithm leverages the fine angular granularity of the calorimeters and the excellent momentum resolution of the inner tracker and muon chambers to greatly improve the reconstruction of physics objects and include soft particles that would otherwise be ignored. This is especially advantageous for jet energy measurements as roughly 62% of the jet energy is carried by charged hadrons, approximately 27% by photons, around 10% by neutral hadrons, and about 1.5% by neutrinos.

The distinguishing feature of the PF algorithm is to combine multiple detector signals together into a single PF candidate. The input detector signals are the tracks,

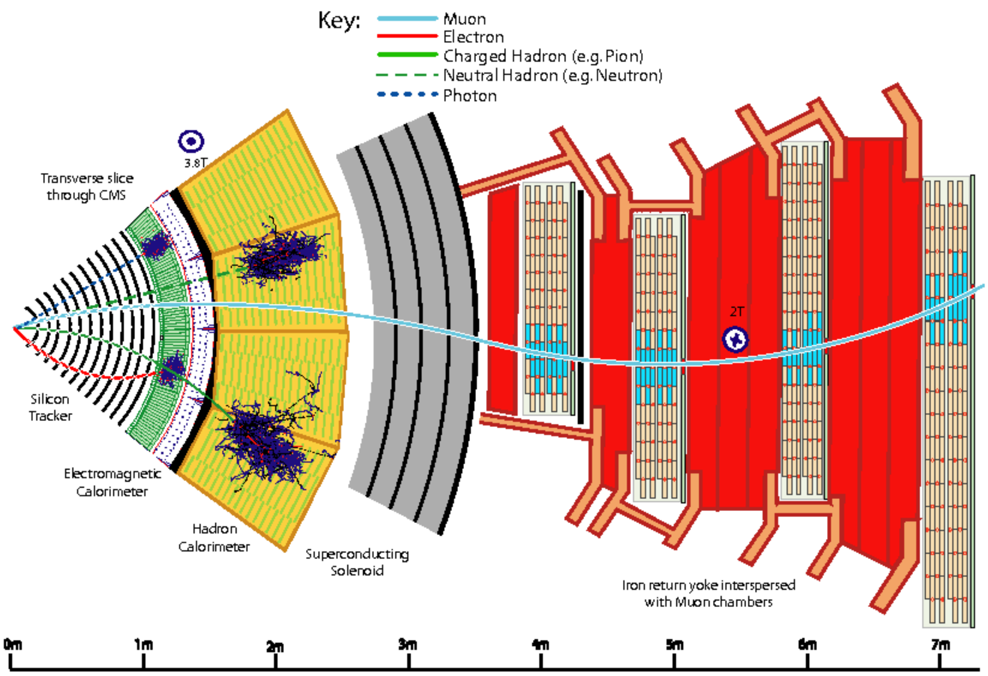

Figure 1-1: A sketch of a transverse slice of the CMS detector showing particle interactions from the interaction point to the muon detector. Reprinted from Reference [].

vertices, calorimeter clusters, and muon segments described in Section 1.1. Based on their proximity in the η-ϕ, these PF elements are combined into muons, electrons, and hadrons. Muon segments are combined with inner tracks to produce muons, inner tracks are combined with calorimeter clusters to produce electrons and charge hadrons, and calorimeter clusters are correlated to produce photons and neutral hadrons.

The PF algorithm reconstructs particles in the blocks described in Section 1.2 and after each block any PF elements associated to a PF candidate are not considered by the following blocks. For example, clusters associated with photons will not be used when reconstructing neutral hadrons. After all PF candidates are identified, they can be combined into event-wide variables such as jets and the missing transverse energy as described in Section 1.3.

1.1 Particle Flow Elements

1.1.1 Tracks

The Combinatorial Track Finder software is used to reconstruct tracks in an iterative inside-out process. Initial interations search for tracks that are easy to find, e.g. those with high p_{T}, and hits associated with these tracks are removed for later iterations, reducing the combinatorial complexity and simplifying the search for more difficult tracks, e.g. greatly displaced ones.

The first step is to form seeds based on pixel hits, double strip hits containing 3D information, and an estimate of the beam spot. Earlier iterations require three pixel hits while later iterations gradually loosen the requirements. The final iterations specifically target increased muon tracking efficiency by including information from the muon chambers.

Next, a Kalman filter is used to find additional hits consistant with the evolution of the track seeds through the rest of the tracker, accounting for the magnetic field, energy loss due to ionization, and multiple scattering. The five parameters used for the helical trajectory evolution are the curvature ρ, the azimuthal angle ϕ_0, the transverse impact parameter d_0 , the longitudinal impact parameter z_0 , and $\lambda = \cot\theta$, where θ is the polar angle.

After propagating the track through all layers of the detector and finding all associated hits, a Kalman fitter and smoother is used to refit the overall trajectory while a fourth-order Runge-Kutta method is used to extrapolate the trajectory between successive hits. To reduce the fraction of fake tracks, various quality requirements concerning the number of missing hits, the reduced χ^2 of the fit, and compatibility with a primary vertex are applied before proceeding to the next iteration.

Track reconstruction for electrons is more complicated as the Kalman filter is not a good description because of the high rate of non-Gaussian energy loss due to brehmsstrahlung these tracks experience within the tracker. To improve the electron reconstruction efficiency, the electron seed collection is filled both by looking outside-in for ECAL superclusters (see Section 1.1.4) consistant with track seeds and inside-out track seeds consistent with superclusters. A Gaussian Sum Filter (GSF) defined to approximate the Bethe-Heitler energy-loss distribution is used to fit the trajectory of electron tracks.

1.1.2 Primary Vertexing

A deterministic annealing (DA) algorithm is used to associate tracks to primary vertices. Tracks must pass additional requirements on the transverse impact parameter d_0, the number of strip and pixel hits, and the reduced χ of the trajectory fit to be considered when finding primary vertices. The most probable vertex positions at an artifical temperature T are determined by the minimization of the "free energy"

$$F = -T \sum_{i}^{N_T} \ln \sum_{j}^{N_V} p_{ij} \rho_j \exp \left[-\frac{1}{T} \left(\frac{z_i^T - z_j^V}{\sigma_i^z} \right)^2 \right] \tag{1.1}$$

where the z_j^V are the vertex positions with weights ρ_j, the z_i^T and σ_i^z are the longitudinal impact parameters and the corresponding uncertainties of the tracks, and the p_{ij} are the probabilities of assigning the track i of N_T to the vertex j of N_V.

The DA algorithm starts with a single vertex at a very high temperature that is gradually decreased. The free energy F is minimized with respects to z_j^K at each new temperature and a vertex is split in two whenever T falls below its criticial temperature

$$T_C^j = 2 \sum_i \frac{p_i p_{ij}}{(\sigma_i^z)^2} \left(\frac{z_i^T - z_j^V}{\sigma_i^z} \right)^2 \Bigg/ \sum_i \frac{p_i p_{ij}}{(\sigma_i^z)^2}. \tag{1.2}$$

The annealing procedure with vertex splitting continues down to $T = 4$ and the final assignment of tracks to vertices is performed at $T = 1$ without any further splitting. The vertex designated as *the* primary vertex of the hard scattering is the one which maximizes

$$\sum_i (p_{\mathrm{T}}^i)^2 + (p_{\mathrm{T}}^{\mathrm{miss}})^2, \tag{1.3}$$

where p_{T}^i is the transverse momentum of a track assigned to the vertex and $p_{\mathrm{T}}^{\mathrm{miss}}$ is the magnitude of the momentum imbalance in the transverse plane for the vertex.

1.1.3 Secondary Vertexing

Long-lived particles such as b hadrons and τ leptons often produce charged particles in their decays. These charged particles are traced to a secondary vertex at the location of the decay, which is identified by the inclusive vertex fitter (IVF) algorithm.

The IVF procedure begins by selecting seed tracks with a 2D impact parameter significance $\sigma_{d_0} \geq 1.2$ and a 3D impact parameter $\sqrt{d_0^2 + z_0^2} \geq 50\,\mu\text{m}$. Tracks are assigned to a secondary vertex based on their opening angle with the seed track and distance at closest approach, with the additional stipulation that this distance be smaller for the secondary vertex than for the primary vertex.

To determine the precise position of the secondary vertices, the associated tracks are fitted with the adaptive vertex fitter and any vertices with a flight distance significance less than a certain threshold are discarded. At this point, a track is unassociated from a secondary vertex if the angular distance between the track and the secondary vertex flight direction is greater than 0.4 and if the track's distance at closest approach is larger than the magnitude of its impact parameter.

The secondary vertex position is refitted after track cleaning if there are still at least two tracks associated with the vertex. The last stage of cleaning removes a secondary vertex if it shares at least 20% of its tracks with another and the flight distance significance between the two is less than ten.

1.1.4 ECAL Superclusters

Due to the large amount of material in the tracker, electrons often emit bremsstrahlung photons, photons often convert to electron-positron pairs, and the brehmsstrahlung photons and converted electrons often undergo further conversion and brehmsstrahlung before reaching the ECAL. Because of the bending of electron trajectories in the magnetic field, the resulting electromagnetic (EM) shower is significantly spread in the ϕ-direction and collimated in the η-direction. The ECAL reconstruction algorithm combines the basic cluster from each showered particle into a supercluster representing the initial electron or photon from the hard scattering.

The first step is the identification of a seed crystal with greater transverse energy than its immediate neighbors and above a predefined minimum threshold. The energy of each crystal is determined from calibration constants combined with the amplitude and peak time obtained by fitting the pulse shape of the ten time samples surrounding the triggering bunch crossing.

In the barrel, a supercluster starts with a 5×1 array of crystals in the η-ϕ plane centred on the seed crystal. The array is extended around the seed crystal in the ϕ-direction up to $|\Delta\phi| \leq 0.3$ if the energy of the additional crystals exceeds a certain threshold. The contiguous array is grouped into distinct basic clusters each containing a seed array with energy greater than another threshold. The supercluster is the collection of basic threshold found in the η-ϕ region centered on the initial seed crystal. Since the crystals in the endcaps are arranged in an x-y grid, clustering here uses fixed 5×5 matrices of crystals. After a seed cluster is identified, additional, partially overlapping 5×5 matrices are added if their centroid lies within $|\Delta\eta| \leq 0.07$ and $|\Delta\phi| \leq 0.3$. For uncoverted photons, both methods produce superclusters that are simple 5×5 matrices.

1.1.5 HCAL Clusters

The purpose of clustering in the HCAL is to measure the energy and direction of neutral hadrons, disentangle neutral hadrons from charged hadron energy deposits, and improve the energy measurement for charged hadrons with poorly reconstructed tracks. Similar to the supercluster algorithm, a cluster in the HCAL is first identified by a seed cell with greater transverse energy than its immediate neighbors and above a predefined minimum threshold. This seed is then grown into a topological cluster by adding cells with at least a corner in common with a cell already in the cluster and energy above twice the noise threshold.

An iterative Gaussian mixture model is used to break each topological cluster of M individual cells is broken into N energy deposits corresponding to individual particles, where N is the number of seeds. Each energy deposit is modeled as a Gaussian distribution $\mathcal{N}$ with amplitude A_i, mean $\vec{\mu}_i$ in the η-ϕ plane, and width

σ fixed by the calorimeter resolution. The expected fraction f_{ji} of the energy E_j measured in the cell at position $\vec{c}_j$ from the ith energy deposit is

$$f_{ji} = \frac{\mathcal{N}\left(\vec{c}_j|A_i, \vec{\mu}_i, \sigma\right)}{\sum_k^N \mathcal{N}\left(\vec{c}_j|A_k, \vec{\mu}_k, \sigma\right)}. \tag{1.4}$$

The amplitude and position of each energy deposit are determined by an analytical maximum-likelihood fit to be

$$A_i = \sum_j^M f_{ji} E_j \;\Bigg|\; \vec{\mu}_i = \sum_j^M f_{ji} E_j \vec{c}_j \tag{1.5}$$

where the initial values are the energy and position of the seeds. The process of calculating energy fractions f_{ji} and fitting for the amplitudes A_i and positions $\vec{\mu}_i$ is repeated until convergence, at which point they are taken as the cluster parameters.

1.1.6 Muon Segments

Muon segments are reconstructed from the hits in the muon chambers using a Kalman filter in a similar manner to that described for the inner tracker in Section 1.1.1. A full track constructed in this way is referred to as a standalone muon.

1.2 Particle Identification

1.2.1 Muons

text.

1.2.2 Electrons

text.

1.2.3 Isolated Photons

text.

1.2.4 Hadrons and Nonisolated Photons

text.

1.3 Event Variables

1.3.1 Jets

1.3.2 Missing Tranverse Energy